Treatment of *Fagus orientalis* Surface by ZnO/TiO₂/FAS-17-Based Nanoparticles

Doğu RAMAZANOĞLU[1*] ⓘ, Ferhat ÖZDEMİR[2] ⓘ

[1]Düzce University, Technology Faculty, Department of Civil Engineering, Düzce, TÜRKİYE
[2]Kahramanmaraş Sütçü İmam University, Faculty of Forstry, Kahramanmaraş, TÜRKİYE
*Corresponding Author: doguramazanoglu@duzce.edu.tr

Abstract

Aim of study: In this research, the surface of *Fagus orientalis* (beechwood) was chosen as a substrate due to its widely used strong biostructure in the wood industry. It was functionalized with ZnO, TiO₂, and FAS-17 nanoparticles to enhance its service life.

Material and methods: FAS-17 (Trimethoxysilane) and ammonium hexafluorotitanate were purchased from Sigma-Aldrich, and zinc borate from Etimine S.A. Methanol, ethyl alcohol, hydrochloric acid, sodium hydroxide, and zinc oxide were provided by TEKKIM. Characterization methods included FTIR, TG/DTA, XRD, SEM, and EDX. Hydrophobicity was determined by water contact angle using KSV Cam101. UV-Vis analysis used a Shimadzu UV-160 spectrophotometer, surface roughness was measured with a Marsurf M 300 device (ISO 4287), and color analysis was performed with a Datacolor Elrepho 450 X spectrometer (ASTM 2021).

Main results: The thermal stability of wood was significantly improved through the hydrothermal deposition of ZnO/TiO₂ nanoparticles. Additionally, hydrophobization was achieved using Triethoxy-1H,1H,1H,2H,2H-perfluorodecylsilane ($C_{14}H_{19}F_{13}O_3Si$), referred to as FAS-17.

Research highlights: The study demonstrated that the introduction of ZnO/TiO₂ nanoparticles improved the thermal stability of wood. Furthermore, the use of FAS-17 resulted in effective hydrophobization. The thermal stability of wood was improved with ZnO/TiO₂ nanoparticles. In addition, hydrophobization was supplied by FAS-17.

Keywords: *Fagus orientalis,* Hydrothermal Method, ZnO/TiO₂/FAS-17 Nano Articles

Fagus orientalis Yüzeyinin ZnO/TiO₂/FAS-17 Bazlı Nanopartiküllerle İşlenmesi

Öz

Çalışmanın amacı: Bu araştırmada, kayın ağacının (*Fagus Orientalis*) yüzeyi, ahşap endüstrisi tarafından yaygın olarak kullanılan güçlü biyoyapısı nedeniyle bir substrat olarak seçilmiştir. Hizmet ömrünü artırmak amacıyla, ZnO, TiO₂ ve FAS-17 nanopartiküller ile fonksiyonelleştirilmiştir.

Materyal ve yöntem: FAS-17 (Trimetoksisilan) ve amonyum hekzaflorotitanat Sigma-Aldrich'ten ve çinko borat Etimine S.A.'dan satın alınmıştır. Metanol, etil alkol, hidroklorik asit, sodyum hidroksit ve çinko oksit TEKKİM tarafından sağlanmıştır. Karakterizasyon yöntemleri arasında FTIR, TG/DTA, XRD, SEM ve EDX yer almıştır. Hidrofobiklik KSV Cam101 kullanılarak su temas açısı ile belirlenmiştir. UV-Vis analizinde Shimadzu UV-160 spektrofotometresi kullanılmış, yüzey pürüzlülüğü Marsurf M 300 cihazı (ISO 4287) ile ölçülmüş ve renk analizi Datacolor Elrepho 450 X spektrometresi (ASTM 2021) ile gerçekleştirilmiştir.

Temel sonuçlar: Ahşabın termal stabilitesi, ZnO/TiO₂ nanopartiküllerin hidrotermal olarak yerleştirilmesiyle önemli ölçüde iyileştirilmiştir. Ayrıca, FAS-17 olarak adlandırılan Triethoxy-1H,1H,2H,2H-perfluorodesilsilan ($C_{14}H_{19}F_{13}O_3Si$) kullanılarak etkili bir hidrofobizasyon sağlanmıştır.

Araştırma vurguları: ZnO tabanlı nano biyomimetik akıllı yüzeyin sentezi, ahşap malzemeye hidrofobik bir özellik kazandırmıştır. Lignoselülozik yüzeyin bu yeni fonksiyonel özelliği, hijyenin önemli olduğu her türlü alanda tercih edilmesini sağlayabilir.

Anahtar Kelimeler: *Fagus Orientalis,* Hidrotermal yöntem, ZnO/TiO₂/FAS-17 Nanoparçacıkları

Introduction

Wood has been used by humans for various purposes since ancient times and is considered one of the oldest materials. Its structure consists of cellulose fibers embedded in a lignin matrix, which gives it unique properties and makes it an intelligent material. Intelligent materials, also known as smart materials, have the ability to respond to external forces and transform them into different energy forms. When the stimuli are removed, they can return to their original state. Examples of smart materials include piezoelectric materials, shape memory alloys, magnetic shape memory materials, and pH-sensitive hydrogels (Qader et al., 2019; Cansiong Guerrra & Escobar Avilés, 2021).

Lignocellulosic materials, including wood, exhibit volume changes in response to moisture. They can expand in moist or aqueous regions and return to their initial state when dried, which classifies them as smart materials (Ugolev, 2014). Wood is highly sought after for its natural, reliable, and aesthetic features in various applications Bennert et al., 2005). However, wood is not resistant to fire, moisture, and light irradiation (Li et al., 2013). Its hydrophilic nature and porous structure make it susceptible to fungi and wood insects (Ramazanoğlu & Özdemir 2022). Therefore, improving its durability, self-cleaning properties, and thermal stability is crucial for expanding its applications and lifespan (Li et al., 2013; Ramazanoğlu & Özdemir, 2022).

Surface coating methods such as impregnation, combining, and synthesis have been used to enhance the thermal stability of wood by applying inorganic materials to the surface (Qu et al., 2021; Niu & Song, 2021; Ramazanoğlu & Özdemir, 2021b ; Ma et al., 2022). The hydrothermal method, which involves physical and chemical interactions, has been utilized to improve the adhesion stability of inorganic materials such as TiO_2, ZnO, and SiO_2 on wooden surfaces (Ali et al., 2021; Kutnar, 2011; Rahimi et al., 2011).

In this research, the hydrothermal method was employed to achieve strong adhesion of ZnO, TiO_2, and FAS-17 nanoparticles to the wood surface. ZnO and TiO_2 nanoparticles were crystallized on the lignocellulosic surface to improve thermal stability.

However, the water contact angle (WCA) results indicated that the surface was more hydrophilic than desired. To address this, FAS-17 was used to reduce the hydrophilic nature caused by ZnO and TiO_2 nanoparticles. Additionally, a low-temperature process was chosen for cost-effectiveness in large-scale applications. A combination of zinc borate and ammonium hexafluorotitanate was used as a source for the aggregation of ZnO, TiO_2 nanoparticles, and FAS-17 on the lignocellulosic surface. These nanoparticles were tested using TGA analysis to assess their effectiveness as intelligent fire barriers. Furthermore, surface hydrophobization was achieved using FAS-17, which has not been extensively studied in the literature.

Material and Methods

Materials

Beech samples were obtained from a commercial market in Kahramanmaraş, Turkey. The reagents used in the experiment included trimethoxysilane (heptadecafluoro-1,1,2,2-tetradecyl) $(CF_3(CF_2)_7CH_2CH_2Si(OCH_3)_3)$, known as FAS-17, and ammonium hexafluorotitanate $(NH4)2TiF6$, both obtained from Sigma-Aldrich. Zinc borate $(2ZnO·3B_2O_3·3.5H_2O)$ was supplied by Etimine S.A. (Battenburg, Luxembourg). Methanol (CH_3OH), ethyl alcohol (EtOH), hydrochloric acid (HCl), sodium hydroxide (NaOH), and zinc oxide (ZnO) were sourced from TEKKIM (Istanbul, Turkey).

Methods

The Fourier transform infrared spectroscopy (FTIR) technique was performed using a Perkin Elmer 400FT-IR/FR-FIR instrument to analyze the wood samples. Thermogravimetric analysis (TGA) was conducted using the Hitachi Exstar and SII TG/DTA 7300 models in a nitrogen atmosphere with a flow rate of 50 ml/min. Approximately 10-11 mg of wood sample was used for three trials. The modification studies were characterized using X-ray diffraction (XRD) with a Rigaku Rint 2000 instrument, scanning electron microscopy (SEM), and energy dispersive X-ray (EDX) analyses with a Zeiss Eva 50 ED instrument. Water contact angle (WCA) was measured using a KSV

Cam101 Scientific Instrument in Helsinki, Finland. The UV-Vis absorption spectra were recorded using a Shimadzu UV-160 spectrometer. Surface roughness analysis was performed using a Mahr Marsurf M 300 device in accordance with ISO 4287 standards.

Color analysis was carried out using a Datacolor Elrepho 450 X device, following the ASTM 2021 standard.

Preparation of Wood Specimens

The wood samples were cut into dimensions of 15 mm (longitudinal) x 10 mm (tangential) x 2 mm (radial), and subsequently, they were washed with distilled water in an ultrasonic bath for 30 minutes. Afterward, the samples were dried in an oven for 2 days at a temperature of 103 ± 2 °C, as illustrated in Figure 1.

Figure 1. Pretreatment of the wood samples

Positioning of ZnO and TiO₂ Nanoparticles On Wood Surface

To precipitate the ZnO/TiO₂ nanoparticles on the lignocellulosic surface, a reaction solution of 50 ml was prepared, consisting of 1.2 M zinc borate ($2ZnO \cdot 3B_2O_3 \cdot 3.5H_2O$) and 0.4 M ammonium hexafluorotitanate (($NH_4)_2TiF_6$), as depicted in Figure 2. The pH of the solution was adjusted to 3 by adding a few drops of a 0.3 M hydrochloric acid solution. Subsequently, the samples were subjected to a hydrothermal treatment for five hours at a temperature of 90 °C, followed by cooling to room temperature (as shown in Fig. 2). Finally, the samples were removed and washed three times using an ultrasonic bath, and then allowed to dry for one day at a temperature of 60 °C (Gao et al., 2015b).

Figure 2. Schematic illustration for the synthesis of the ZnO and TiO₂ nanoparticles on the wood surface using a hydrothermal treatment

Hydrophobization of ZnO/TiO₂ Treated Wood Samples by FAS-17

To hydrophobize the surface, a solution was prepared by combining 20 ml of methanol with 0.20 ml of FAS-17. The solution was then hydrolyzed by adding 60 ml of distilled water. Subsequently, the wood samples treated with ZnO/TiO₂ were immersed in this solution for a hydrothermal process lasting five hours at a temperature of 80 °C (as shown in Fig. 3). After the hydrothermal treatment, the reactor was cooled to room temperature, and the samples were removed and washed with ethyl alcohol to eliminate any unreacted agents. Finally, the wood samples were dried at 60 °C for 24 hours until the ethyl alcohol had evaporated, resulting in a hydrophobic surface (Gao et al., 2015b).

Figure 3. Schematic representation of the hydrophobization

Results and Discussion

Analysis of the X-ray Diffraction (XRD) Spectra

The X-ray diffraction (XRD) spectra of the wood samples treated with the hydrothermal process using the reactor solution containing 0.4 M ammonium hexafluorotitanate and 1.2 M zinc borate are presented in Figure 4. The characteristic peaks of untreated wood are shown in Figure 4a, and they appear at 16.4° and 22.5°, which can be attributed to cellulose (Burhenne et al., 2013; Yeo et al., 2019; Báder at al., 2020; Xiang et al., 2021).
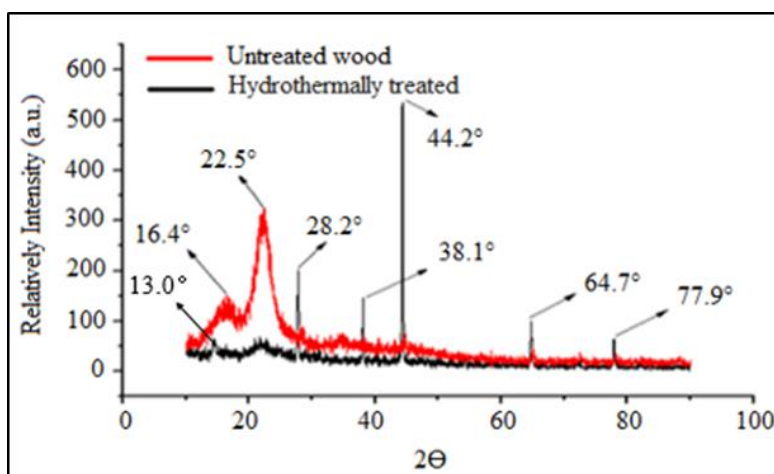

Figure 4. XRD spectrum of untreated and treated wood samples

After the hydrothermal treatment, the XRD peaks observed at 13.0°, 21.7°, 28.2°, 38.1°, 44.2°, 64.7°, and 77.9° indicate the presence of crystal structures on the wood surface (Hsieh et al., 2022; Beyene etal., 2020). These peaks are indicative of the presence of ZnO and TiO_2 nanoparticles on the wood surface. Different forms of TiO_2 have been discussed in the literature, and distinguishing between them can be challenging. The anatase and rutile structures have characteristic reflection peaks around 2θ values of 25.28° (d101 of anatase) and 27.4° (d110 of rutile), respectively. On the other hand, distinguishing between anatase and brookite can be more difficult as their peaks are closer together. The brookite phase exhibits a peak at approximately 2θ = 30.81° (d121), while the anatase phase exhibits a peak at around 2θ = 62.57° (d204) (Di Paola et al., 2013).

Based on the provided references (Aad et al., 2013; Cui et al., 2017; Nakayasu et al., 2022), Figure 4 displays the XRD spectra of both untreated and hydrothermally treated wood samples at 90 °C for 5 hours. It has been noted by Di Paola et al. (2013) that TiO_2 nanoparticles can exist in various polymorphic forms. The peaks observed at 13.0°, 28.2°, and 38.1° in the XRD spectra correspond to the ZnO hexagonal wurtzite structure, as indicated by the JCPDS card 36-1451 (Sun et al., 2013). As mentioned earlier, XRD is a valuable technique that can differentiate between different polymorphic forms of TiO_2, and specific peak angles can provide information about the presence of particular forms of TiO_2 or ZnO.

Scanning Electron Microscopy (SEM) and Energy Dispersive X-ray (EDX) Analysis

Figure 5 showcases SEM photos and EDX spectra of three different samples: untreated wood (a), wood treated with ZnO microparticles and TiO_2 nanoparticles (b), and hydrophobized ZnO/TiO_2 treated wood (c).
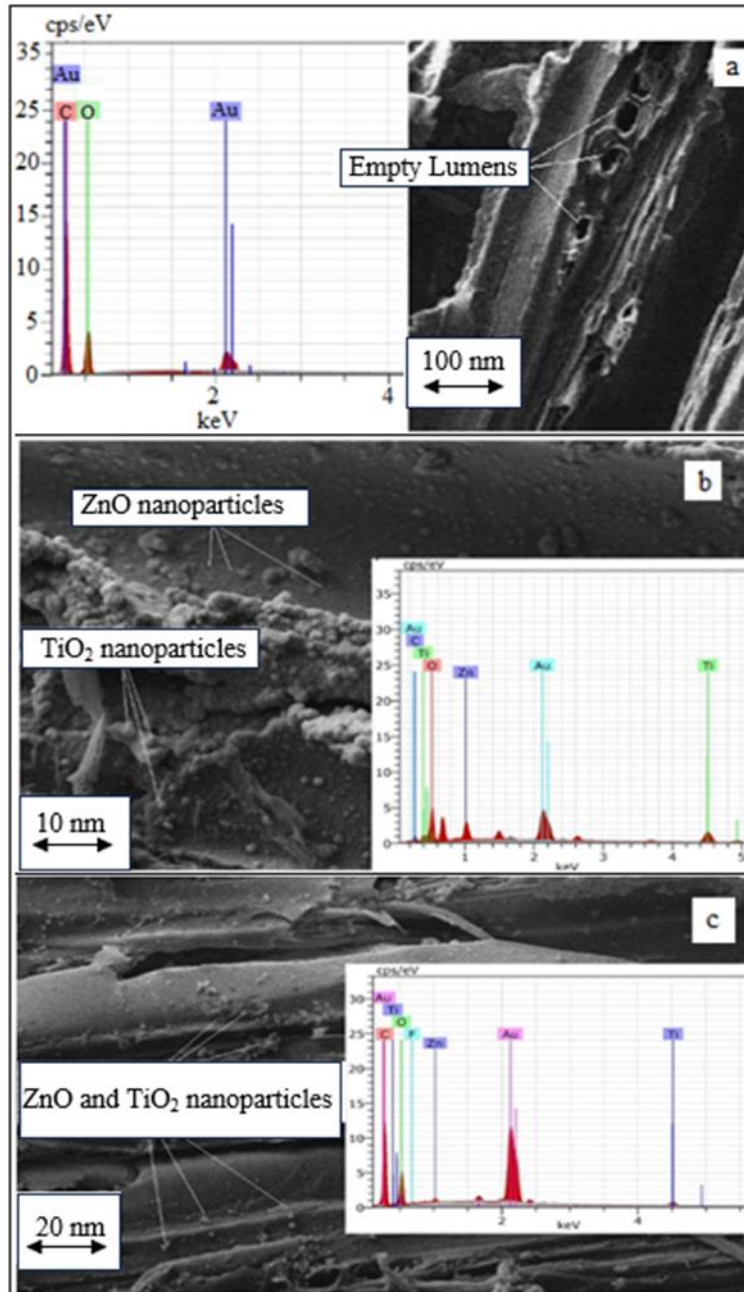

Figure 5. The SEM images and EDX spectrums of (a) native wood; (b) ZnO/TiO_2 treated wood; and (c) hydrophobized ZnO/TiO_2 treated wood via FAS-17

In Fig. 5a, the EDX spectrum of untreated wood exhibits peaks corresponding to carbon and oxygen, indicating the presence of the cellulosic structure, as well as gold peaks attributed to surface coating. Fig. 5b's EDX spectrum indicates the presence of peaks related to titanium (Ti) and zinc (Zn), indicating the coverage of ZnO and TiO_2 nanoparticles on the wood surface (Gao et al., 2015a). Fig. 5c's EDX spectrum shows peaks corresponding to titanium (Ti) and zinc (Zn), suggesting the functionalization of FAS-17 on the wood surface (Gao et al., 2015a). From the SEM images, it can be observed that grass-like ZnO nanoparticles are present in Fig. 5b (Li et al., 2013). However, in Fig. 5c, wax crystalloids covering the ZnO/TiO_2 nanoparticles are not visible due to insufficient magnification.

Thermogravimetric Analysis (TGA)

Figure 6 illustrates the thermogravimetric (TG) and derivative TG (DTG) plots for samples treated with FAS-17 and the reactor solution containing zinc borate ($2ZnO·3B_2O_3·3.5H_2O$) and ammonium hexafluorotitanate ($(NH_4)_2TiF_6$).

In the TG curves, similar behavior is observed up to 100 °C, which can be attributed to the removal of water from the samples (Zhai et al., 2016). The DTG plot shows a shoulder at 295 °C (Fig. 6a), indicating hemicellulose depolymerization, while thermal decomposition of cellulose occurs at 359 °C (Ouajai & Shanks, 2005). In the DTG plot, distinct and sharp endothermic peaks are observed at 338 °C for the wood treated with ZnO/TiO_2 and at 390 °C for the hydrophobized wood via FAS-17 (Figs. 6b and 6c). These peaks correspond to the weight losses observed in the TG curve. It is noted that the untreated sample experiences a higher weight loss. The depolymerization of FAS-17 acts as a protective barrier for the wood, while the ZnO and TiO_2 nanoparticles act as catalysts, accelerating the pyrolysis time by forming a protective layer on the wood surface. The combined effect of ZnO/TiO_2 and FAS-17 contributes to catalysis, resulting in reduced pyrolysis time. After combustion, the untreated sample loses 98.7% of its weight, whereas the ZnO/TiO_2 treated sample loses 85.0% and the $ZnO/TiO_2/FAS-17$ treated wood loses 54.5% of its weight.

These TG and DTG plots provide insights into the thermal behavior of the samples, highlighting the protective and catalytic effects of ZnO/TiO_2 nanoparticles and FAS-17 treatment on wood decomposition.
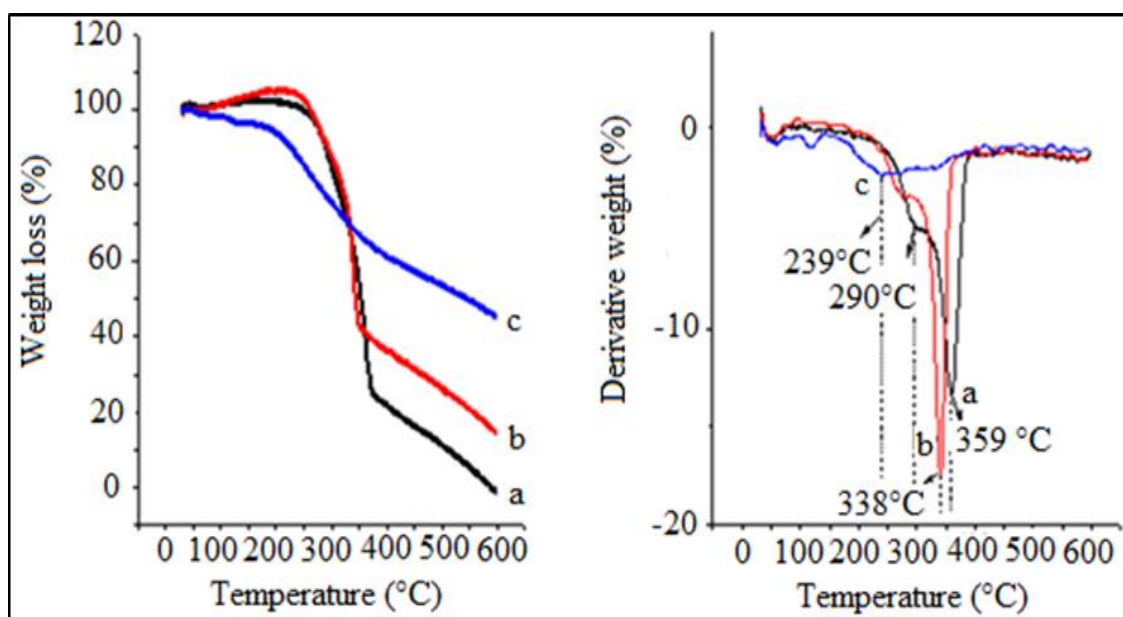

Figure 6. The thermogravimetric analysis (TG/DTG) spectrum of the (a) solid wood; (b) ZnO/TiO_2 treated wood; and (c) hydrophobized ZnO/TiO_2 treated wood via FAS-1

Surface Roughness

The hydrothermal method operates as a closed system, enabling reactions to occur under pressure within a temperature range suitable for crystallization on the lignocellulosic surface. Moreover, it offers a cost-effective approach for large-scale production. Following the attachment of TiO_2 and ZnO nanoparticles onto the surface through hydrothermal treatment, the surface roughness parameters (Ra, Rz, and Rmax) exhibited significant increases of 148%, 130%, and 156%, respectively (as shown in Fig. 7a). Additionally, when the samples underwent ultrasonic baths (as shown in Fig. 7b), their surface parameters increased by 107%, 104%, and 122%, respectively. These changes in surface roughness resulted from the formation of cavities within the wood cells and channels subsequent to the ultrasonic baths (Özdemir et al., 2018a;b; Ramazanoğlu & Özdemir, 2019; Ramazanoğlu & Özdemir, 2020a;b).
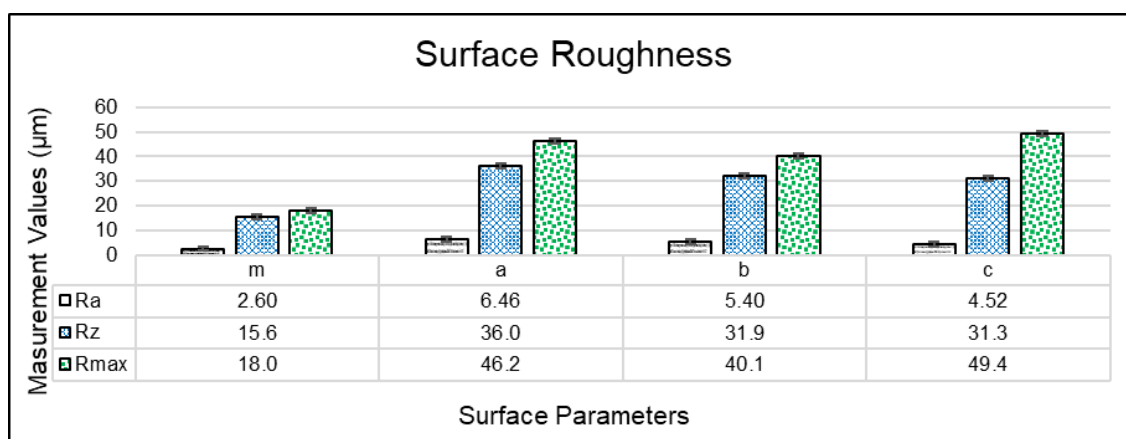

Figure 7. The surface roughness parameters of the (m) native wood; (a) ZnO-TiO_2 treated (without ultrasonic bath; (b) ZnO-TiO_2 treated wood; and (c) ZnO/TiO_2/FAS-17 treated wood.

Upon hydrophobization of sample b using FAS-17 (as shown in Fig. 7b), the Ra and Rz values decreased by 16.2% and 1.88%, respectively, while the Rmax values increased by 23.1%. The initial increases in roughness, without hydrophobization and after the ultrasonic bath, are attributed to the accumulation of ZnO and TiO_2 nanostructures on the solid surface (Gao et al., 2015; Ramazanoğlu, 2020; Ramazanoğlu & Özdemir, 2022). Notably, alterations in the surface parameters subsequent to hydrophobization with FAS-17, which acts as a final layer covering other nanoparticles, play a vital role in achieving water repellency (Li et al., 2013; Huang et al., 2011; Özdemir et al., 2018a; b). Such nanostructures are observed on the leaves of hydrophobic plants, such as lotus and rose (Ramazanoğlu & Özdemir, 2021a; b).

Color Analysis

Figure 8 illustrates the comparison between massive wood (m), ZnO/TiO_2-treated wood (a), and ZnO/TiO_2-treated wood hydrophobized by FAS-17 (b). The color parameters, namely yellowness, brightness, and whiteness, were measured for the solid wood (m) and determined to be 27.5%, 32.7%, and 39.8%, respectively. For the ZnO/TiO_2-treated surface (b), these parameters were found to be 28.6%,26.3%, and 32.2%, respectively. After the hydrophobization with FAS-17 (c), the color parameters were measured as 34.9%, 27.6%, and 36.1%, respectively. These changes in color following each treatment (as shown in Fig. 9a) indicate the successful presence of ZnO, TiO_2, and FAS-17 nanoparticles on the wood surface (Özdemir et al., 2018b; Ramazanoğlu & Özdemir, 2019; 2020b; 2022; 2023)
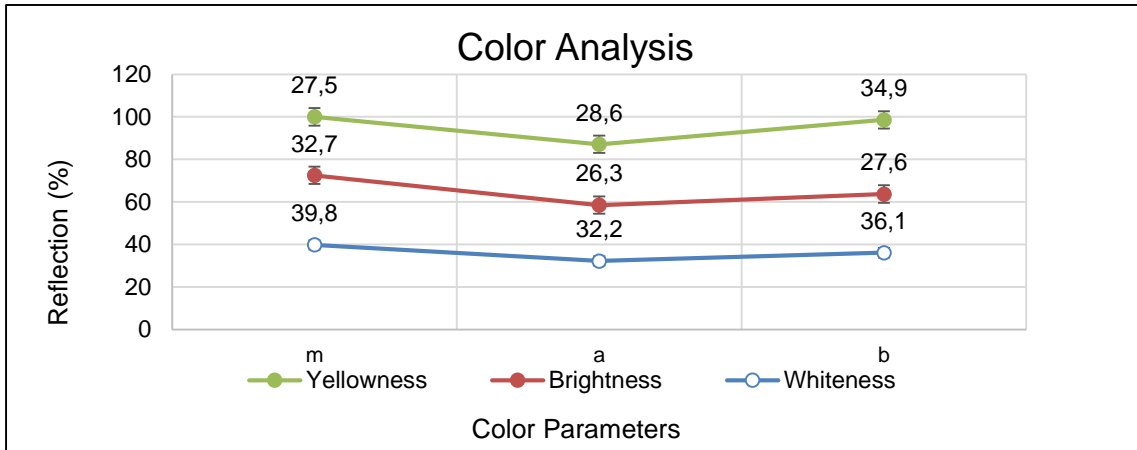
Figure 8. The color parameters of massive wood (m), ZnO/TiO_2 treated-wood (a), and (b) ZnO/TiO_2@FAS-17-treated wood

Figure 9. The color parameters of massive wood (m), ZnO/TiO_2 treated-wood (a), and ZnO/TiO_2@FAS-17-treated wood (b)

Water Contact Angles

The water contact angles of massive wood after each treatment step have given in Fig. 10.
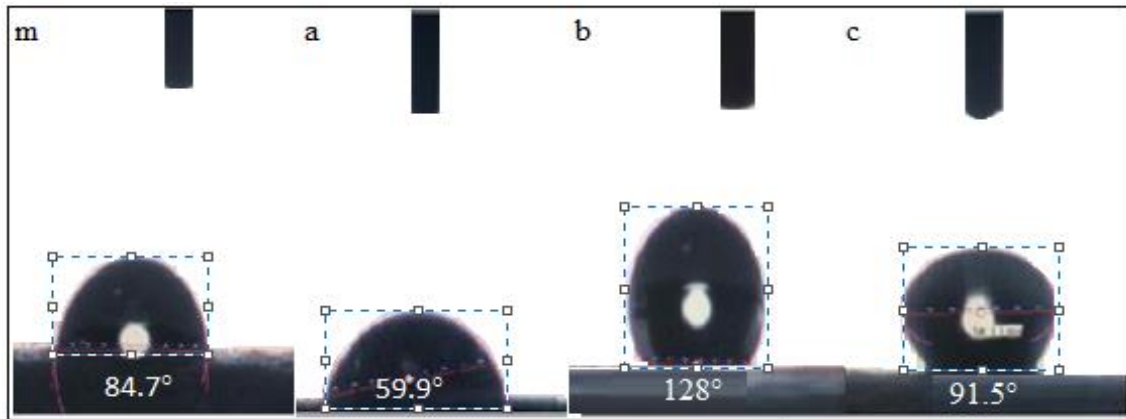

Figure 10. Massive wood (m), ZnO/TiO_2-treated wood (b), FAS-17 (c), and (d) ZnO/TiO_2/FAS-17 treated wood

The water contact angle (WCA) of the massive wood was initially measured at $\theta\gamma$ 84.7° before the hydrothermal reaction. After exposure to the $[2ZnO \cdot 3B_2O_3 \cdot 3.5H_2O /(NH_4)_2TiF_6]$ reaction solution, the WCA value decreased by 29.3% and was measured as $\theta\gamma$ 59.9°. This decrease indicates the functionalization of ZnO/TiO_2 nanoparticles on the wood surface (Gan et al., 2015; Cui et al., 2017; Ramazanoğlu & Özdemir, 2022).

The wood surface treated with FAS-17 obtained a water contact angle of $\theta\gamma$ 128° (Figure 10.c). After the hydrophobization of the ZnO/TiO_2-treated wood with FAS-17, the water contact angle increased by 52.7% and was recorded as $\theta\gamma$ 91.5° (Fig 10.d.).

Conclusion

Wood, as one of the earliest materials utilized by humans for various purposes, such as heating, hunting, and shelter, has been a popular choice in human living spaces. Its naturalness, easy availability, and functionality have made it a preferred material. However, wood has inherent weaknesses, particularly in terms of its resistance to fire and water. Therefore, this study aimed to enhance the water and thermal resistance of wood.

Based on the obtained data, it was observed that the thermal stability of the wood improved by 45.5%. Additionally, the surface hydrophobicity was enhanced by 8.02%. These improvements are significant in increasing the longevity and durability of wood and wood-based materials. Further research should focus on exploring the functionalization of the wood surface under optimal nanoparticle synthesis conditions. This can contribute to extending the service life of wood and wood-based materials.

The multifunctionalization of wood surfaces can have several benefits. It can reduce maintenance costs and minimize the extensive use of chemicals to protect wood-based materials from outdoor conditions. Furthermore, this approach can have positive environmental implications by reducing chemical usage. By enhancing the resistance of wood to water and thermal degradation, we can promote sustainable and long-lasting utilization of this valuable natural resource.

Ethics Committee Approval
N/A

Peer-review
Externally peer-reviewed.

Author Contributions

Conceptualization: D.R.; Investigation: D.R.; Material and Methodology: D.R.; Supervision: F.Ö. Visualization: D.R.; Writing-Original Draft: D.R.; Writing-review & Editing: D.R. All authors have read and agreed to the published version of manuscript.

Conflict of Interest

The authors have no conflicts of interest to declare.

References

Aad, R., Simic, V., Cunff, L. L., Rocha, L., Sallet,V., Sartel, C., Lusson, A., Couteaua, C. & Lerondel, G. (2013). ZnO nanowires as effective luminescent sensing materials for nitroaromatic derivatives. *Nanoscale,* 5, 9176-9180.

Ali, M. R., Abdullah, U. H., Ashaari, Z., Hamid, N. H., & Hua, L. S. (2021). Hydrothermal Modification of Wood: A Review. *Polymers,* 13(16), 2612.

ASTM, Standard Practice for Calculation of Color Tolerances and Color Differences from Instrumentally Measured Color Coordinates. (2021).

Báder, M., Németh, R., Sandak, J., & Sandak, A. (2020). FTIR analysis of chemical changes in wood induced by steaming and longitudinal compression. *Cellulose,* 27(12), 6811-6829.

Bennert, T., Hanson, D., Maher, A. & Vitillo, N. (2005). Influence of pavement surface type on tire/pavement generated noise. *Journal of Testing and Evaluation,* 33 (2), 94-100.

Beyene, D., Chae, M., Vasanthan, T., & Bressler, D. C. (2020). A Biorefinery Strategy That Introduces Hydrothermal Treatment Prior to Acid Hydrolysis for Co-generation of Furfural and Cellulose Nanocrystals. Frontiers in Chemistry, 8.

Burhenne, L., Messmer, J., Aicher, T., & Laborie, M. P. (2013). The effect of the biomass components lignin, cellulose, and hemicellulose on TGA and fixed bed pyrolysis. *Journal of Analytical and Applied Pyrolysis,* 101, 177-184.

Cansiong Guerrra, K. S. & Escobar Avilés, J. (2021). The use of wood as Smart Building Material = El uso de la madera como Smart Building Material. *Building & Management*, 4(1), 36.

Cui, W., Zhang, N., Xu, M., & Cai, L. (2017). Combined effects of ZnO particle deposition and heat treatment on dimensional stability and mechanical properties of poplar wood. Scientific Reports, 7(1).

Gan, W., Gao, L., Sun, Q., Jin, C., Lu, Y., & Li, J. (2015). Multifunctional wood materials with magnetic, superhydrophobic and anti-ultraviolet properties. *Applied Surface Science,* 332, 565-572.

Gao, L., Lu, Y., Zhan, X. & Sun, Q. (2015a). A robust, anti-acid, and high-temperature humidity-resistant superhydrophobic surface of Wood based on a modified TiO₂ film by fluoroalkyl silane. *Surface and Coatings Technology,* 262, 33-39.

Gao, L., Xiao, S., Gan, W., Zhan X. & Li, J., (2015b). Durable superamphiphobic wood surfaces from Cu2O film modified with fluorinated alkyl silane. *Royal Society of Chemistry*, 5, 98203-98208.

ISO 4287, (1997). Geometrical Product Specifications Surface Texture Profile Method Terms. Definitions and Surface Texture Parameters, International Standard Organization.

Kutnar, A. (2011). Adhesive bonding of hydrothermally modified wood. Adhesive Properties in Nanomaterials, Composites and Films, 71-82.

Li, N., Xia, T., Heng, L. & Liu, L. (2013). Superhydrophobic Zr-based metallic glass surface with high adhesive force. Applied Physics Letters, 102(25), 251603.

Ma, G., Wang, X., Cai, W., Ma, C., Wang, X., Zhu, Y., Kan, Y., Xing, W., & Hu, Y. (2022). Preparation and Study on Nitrogen- and Phosphorus-Containing Fire Resistant Coatings for Wood by UV-Cured Methods. Frontiers in Materials, 9.

Niu, K., & Song, K. (2021). Surface coating and interfacial properties of hot-waxed wood using modified polyethylene wax. Progress in Organic Coatings, 150, 105947.

Huang, S., Hu, Y., & Pan, W. (2011). Relationship between the structure and hydrophobic performance of Ni–TiO2 nanocomposite coatings by electrodeposition. Surface and Coatings Technology, 205(13–14), 3872–3876.

Ouajai, S., & Shanks, R. A. (2005). Composition, structure, and thermal degradation of hemp cellulose after chemical treatments. Polymer Degradation and Stability, 89(2), 327-335.

Özdemir, F., Ramazanoğlu, D., & Tutuş A. (2018b). Göknar odunun yüzey kalitesi üzerine yaşlandırma süresi, zımparalama ve kesit yönü etkisinin araştırılması [Investigation of the effect of aging time, sanding, and cross-section on the surface quality of fir wood] Bartın Orman Fakültesi Dergisi, 20(2), 194-204.

Özdemir, F., Ramazanoğlu, D., & Tutuş, A. (2018a). Akıllı malzemeler için biyomimetik yüzey tasarımları [Biomimetic surface designs for smart materials] Journal of Bartin Faculty of Forestry 20(3), 664-676.

Qader I.N., Kok M., Dagdelen F., Aydogdu Y, (2019). "A review of smart materials: researches and applications," El-Cezerî Journal of Science and Engineering, 6(3); 755-788

Qu, L., Rahimi, S., Qian, J., He, L., He, Z., & Yi, S. (2021). Preparation and characterization of hydrophobic coatings on wood surfaces by a sol-gel method and post-aging heat treatment. Polymer Degradation and Stability, 183, 109429.

Rahimi, A. R., Modarress, H., and Iranagh, S. A. (2011) Effect of alumina nanoparticles as nanocomposites on morphology and corrosion resistance of electroless Ni–P coatings," Surface Engineering 27(1) 26-31.

Ramazanoğlu, D., & Özdemir, F. (2023). Sürdürülebilir ahşap koruma için nanoteknoloji potansiyelinin araştırılması. Turkish Journal of Forestry, 24(2), 122-133.

Ramazanoğlu, D., & Özdemir, F. (2019). Lignocellulosic-based smart landscape composites, in: Proceedings of the III. International Mediterranean Forest and Environment Symposium, Kahramanmaraş, Turkey, 637-642.

Ramazanoğlu, D., & Özdemir, F. (2020). Hidrotermal yaklaşımın lignoselülozik yüzeydeki akıllı nano biyomimetik yansıması, Turkish Journal of Forestry, 21(3), 324-33.

Ramazanoğlu, D., & Özdemir, F. (2020a). Ön işlem olarak uygulanan ultrasonik banyonun ceviz kaplamaların özellikleri üzerine etkileri *Bartın Orman Fakültesi Dergisi,* 22(2), 479-484.

Ramazanoğlu, D., & Özdemir, F. (2021b). Intelligent biomimetic artificial form for lignocellulosic surfaces. *Kastamonu University Journal of Forestry Faculty,* 21(2), 95-103.

Ramazanoğlu, D., & Özdemir, F. (2022). Biomimetic surface accumulation on Fagus orientalis. *Applied Nanoscience,* 12, 2421-2428.

Ramazanoğlu, D., & Özdemir. F., (2020b). Hidrotermal yaklaşımın lignoselülozik yüzeydeki akıllı nano biyomimetik yansıması *Turkish Journal of Forestry,* 21(3), 324-331.

Ramazanoğlu, D. (2020). Akıllı Biyomimetik Nano Hibrit Yüzey Formlarının Tasarımı ve Lignoselülozik Yüzeyde Hidrotermal Modifikasyonunun İncelenmesi Ph.D. Dissertation, Kahramanmaraş Sütçü İmam Üniversitesi, Kahramanmaraş, Turkey.

Ramazanoğlu. D. & Özdemir, F. (2021a). ZnO-based nano biomimetic smart artificial form located on lignocellulosic surface with hydrothermal approach. Kastamonu University Journal of Forestry Faculty, 21(1), 12-20.

Hsieh, M.-C., Hung, K.-C., Xu, J.-W., Wu, Y.-H., Chang, W.-S., & Wu, J.-H. (2022). Characterization and Prediction of Mechanical and Chemical Properties of Luanta Fir Wood with Vacuum Hydrothermal Treatment. *Polymers,* 15(1), 147.

Nakayasu, Y., Goto, Y., Katsuyama, Y., Itoh, T.,

& Watanabe, M. (2022). Highly crystalline graphite-like carbon from wood via low-temperature catalytic graphitization. *Carbon Trends,* 8, 100190.

Sun, Y. X., Wang, L., Dong, X. Y., Ren, Z. L. & Meng, W. S. (2013). Synthesis, characterization, and crystal structure of a supramolecular CoII complex containing Salen-type bisoxime. Synthesis and Reactivity in Inorganic, Metal-Organic, and Nano-Metal Chemistry, 43(5), 599-603.

Ugolev, B. N. (2006). Frozen strains of wood as natural intelligent material. In: Proceedings of 5th IUFRO symposium wood structure and properties, Zvolen, Slovakia, 423-426.

Ugolev, B. N. (2014). Wood as a natural smart material. *Wood Science Technology,* 48, 553-568.

Xiang, E., Huang, R., & Yang, S. (2021). Change in Micromechanical Behavior of Surface Densified Wood Cell Walls in Response to Superheated Steam Treatment. *Forests,* 12(6), 693.

Yeo, J. Y., Chin, B. L. F., Tan, J. K., & Loh, Y. S. (2019). Comparative studies on the pyrolysis of cellulose, hemicellulose, and lignin based on combined kinetics. Journal of the Energy Institute, 92(1), 27-37.

Zhai, M., Guo, L., Zhang, Y., Dong, P., Qi, G., and Huang, Y. (2016). Kinetic parameters of biomass pyrolysis by TGA, *BioRes.* 11(4), 8548-8557.